J. Cell. Mol. Med. Vol 13, No 10, 2009 pp. 4192-4204

Haemopexin affects iron distribution and ferritin expression in mouse brain

Noemi Morello [a], Elisabetta Tonoli [b], Federica Logrand [a], Veronica Fiorito [a], Sharmila Fagoonee [a], Emilia Turco [a], Lorenzo Silengo [a], Alessandro Vercelli [b], Fiorella Altruda [a], Emanuela Tolosano [a, *]

[a] Molecular Biotechnology Center, University of Torino, Torino, Italy
[b] Department of Anatomy, Pharmacology and Forensic Medicine, University of Torino, Torino, Italy

Abstract

Haemopexin (Hx) is an acute phase plasma glycoprotein, mainly produced by the liver and released into plasma where it binds heme with high affinity and delivers it to the liver. This system provides protection against free heme-mediated oxidative stress, limits access by pathogens to heme and contributes to iron homeostasis by recycling heme iron. Hx protein has been found in the sciatic nerve, skeletal muscle, retina, brain and cerebrospinal fluid (CSF). Recently, a comparative proteomic analysis has shown an increase of Hx in CSF from patients with Alzheimer's disease, thus suggesting its involvement in heme detoxification in brain. Here, we report that Hx is synthesised in brain by the ventricular ependymal cells. To verify whether Hx is involved in heme scavenging in brain, and consequently, in the control of iron level, iron deposits and ferritin expression were analysed in cerebral regions known for iron accumulation. We show a twofold increase in the number of iron-loaded oligodendrocytes in the basal ganglia and thalamus of Hx-null mice compared to wild-type controls. Interestingly, there was no increase in H- and L-ferritin expression in these regions. This condition is common to several human neurological disorders such as Alzheimer's disease and Parkinson's disease in which iron loading is not associated with an adequate increase in ferritin expression. However, a strong reduction in the number of ferritin-positive cells was observed in the cerebral cortex of Hx-null animals. Consistent with increased iron deposits and inadequate ferritin expression, malondialdehyde level and Cu–Zn superoxide dismutase-1 expression were higher in the brain of Hx-null mice than in that of wild-type controls. These data demonstrate that Hx plays an important role in controlling iron distribution within brain, thus suggesting its involvement in iron-related neurodegenerative diseases.

Keywords: haemopexin • heme • iron • oligodendrocyte

Introduction

Iron is an essential cofactor for many proteins that are involved in the normal function of neuronal tissue, such as enzymes involved in neurotransmitter synthesis and myelination of axons [1]. However, there is increasing evidence that iron is involved in the mechanisms underlying many neurodegenerative diseases. Pathological conditions such as neuroferritinopathy and Friedreich ataxia are associated with mutations in genes that encode proteins involved in the control of iron homeostasis [2, 3]. Moreover, during aging, iron accumulates in brain regions that are affected by Alzheimer's disease and Parkinson's disease. High concentrations of reactive iron can increase oxidative stress-induced neuronal vulnerability, and iron accumulation might increase the toxicity of environmental or endogenous toxins [4].

Haemopexin (Hx) is an acute phase plasma glycoprotein with a high heme binding affinity ($K_d < 10^{-9}$ M). Hx is mainly produced by the liver and released into plasma where it binds heme and delivers it to the liver [5]. Accordingly, it has been demonstrated that, after injection of labelled heme-Hx complexes into rats, heme accumulates in the liver and heme-derived iron associates to ferritin [6, 7]. *In vitro* data have shown that the heme-Hx complex is able to induce the expression of heme oxygenase (HO)-1 and to activate cellular protection mechanisms [8, 9].

Thus, Hx provides protection against free heme-mediated oxidative stress [10, 11], limits access by pathogens to heme [12] and contributes to iron homeostasis by recycling heme iron [13]. Consistently, Hx-null mice recover less efficiently than wild-type controls after acute haemolysis and suffer from severe renal damage due to iron overload and oxidative injury [14]. Moreover,

*Correspondence to: Emanuela TOLOSANO, Ph.D., Molecular Biotechnology Center, Department Genetics, Biology and Biochemistry, Via Nizza 52, 10126 Torino, Italy.
Tel.: +39-011-6706423
Fax: +39-011-6706432
E-mail: emanuela.tolosano@unito.it

doi:10.1111/j.1582-4934.2008.00611.x

© 2008 The Authors
Journal compilation © 2009 Foundation for Cellular and Molecular Medicine/Blackwell Publishing Ltd

compound mutant mice for Hx and its closely related protein, haptoglobin showed marked liver inflammation and fibrosis after haemolytic stress [15].

Other than in plasma and liver, Hx protein has been found in the sciatic nerve, skeletal muscle, retina and brain [16–19]. Moreover, human Hx promoter activity has been reported in several brain regions in transgenic mice, including cortex, hippocampus, thalamus, hypothalamus, cerebellum and brainstem nuclei [20, 21]. Recently, Hx has been identified in human cerebrospinal fluid (CSF), and a comparative proteomic analysis has demonstrated a significant increase in Hx levels in CSF from Alzheimer's disease patients compared to non-demented elderly persons [22, 23]. However, it remains unclear whether Hx is locally synthesized in extra-hepatic tissues or it is taken up from plasma.

Data on Hx expression in brain and its modulation under pathological conditions suggest that it might act as heme scavenger and protective factor in the nervous system as well. To test this hypothesis, we analysed iron deposits, ferritin expression and oxidative stress in the brain of Hx-null mice.

Materials and methods

Animals

Hx-null mice were generated in our laboratory as previously described [14]. Two-month-old $Hx^{-/-}$ and $Hx^{+/+}$ mice used for experiments were in the 129Sv genetic background and were maintained on a standard diet. For the production of an anti-Hx antibody, $Hx^{-/-}$ mice in C57BL/J6 background were immunized with a recombinant Hx protein (see next paragraph). All experiments were approved by the animal studies committee of the University of Torino (Italy).

Production of anti-haemopexin antibodies

Polyclonal and monoclonal antibodies were produced against a recombinant protein obtained in *E. coli* and corresponding to amino acids 81–459 of mouse Hx. This sequence was sub-cloned from a full-length murine Hx clone (NP_059067) purchased from Invitrogen (San Giuliano Milanese, MI, Italy). The recombinant Hx protein was injected in Hx-null mice of C57BL/J6 background, and the resulting antibodies were characterized by Western blotting using plasma from wild-type mice. Plasma from Hx-null mice was used as negative control. To test for antibody specificity, pre-adsorption with recombinant Hx was performed. Two monoclonal antibodies (1B5/D4 and 3D6/E12) were thus obtained.

Tissue and serum iron measurement

Mice were anaesthetized with Avertin (2,2,2-tribromoethanol; Sigma-Aldrich, Milano, Italy) at a dose of 2 mg/kg body weight and transcardially perfused with 0.1 M phosphate-buffered saline (PBS), and tissue non-heme iron content determined with a colorimetric method using 4,7-diphenyl-1, 10-phenantroline disulphonic acid (BPS) as chromogen [24]. Briefly, 0.1 g of dry tissue was incubated overnight in a mixture of trichloroacetic (10%) and hydrochloric (4N) acids, and 100 μl of supernatant reduced with thioglycolic acid (Sigma-Aldrich) and acetic acid-acetate buffer (pH 4.5). Ferrous iron content was determined spectrophotometrically at 535 nm following addition of BPS and incubation for 1 hr at 37°C. Results were expressed as μg iron/g dry tissue weight.

Serum iron and unsaturated iron-binding capacity (UIBC) were measured in non-haemolysed mouse serum using a Randox iron/TIBC (total iron-binding capacity) Reagent Set according to the manufacturer's instructions (Randox, Ardmore, UK). TIBC and transferrin saturation were calculated from measured serum iron and UIBC.

Histology

Animals were anaesthetized as described above and transcardially perfused with 0.1 M PBS, pH 7.2 followed by fixative solution (4% paraformaldehyde in PBS). Brains were post-fixed in the same fixative (4 hrs at 4°C), washed in PBS, cryoprotected by immersion in 30% sucrose in PBS overnight, embedded and frozen in cryostat medium (Bio-Optica, Milano, Italy). The brain was cut in coronal 50-μm-thick, free-floating sections which were stored in a cryoprotective solution at −20°C until processed for iron staining, X-Gal staining, immunohistochemistry and immunofluorescence.

Iron staining and image analysis

Iron was detected on brain sections using Perl's staining for non-heme ferric iron (Fe(III)) followed by DAB (methanol 3,3 diamino-benzidine, Roche, Milano, Italy) development according to standard protocols. Briefly, free-floating tissue sections were rehydrated in PBS, incubated in 0.3% hydrogen peroxide in PBS, washed in PBS and subsequently incubated with Perl's solution (1% potassium ferrocyanide and 1% HCl in PBS), followed by incubation with DAB and hydrogen peroxide for 15 min. Sections were then transferred on gelatin-coated slides, rinsed in PBS, counterstained with haematoxylin, dehydrated and mounted in DPX (BDH Laboratory Supplies, Leicester, UK). Quantification of iron positive cells was performed with a computer-microscope system equipped with the NeuroLucida program (Microbrightfield, Inc., Williston, VT, USA). Positive cells were counted on four 50-μm-thick serial sections obtained every 0.3 mm through the basal ganglia and thalamus, for each animal. Four mice for each genotype were analysed.

X-Gal staining

Brain sections were washed in PBS and transferred into X-Gal staining solution [0.5 mg/ml of 5-bromo-4-chloro-3-indolyl β-D-galactoside (X-Gal), 2 mM $MgCl_2$, 5 mM potassium ferrocyanide, 5 mM potassium ferricyanide, 0.01% Triton-X-100 in PBS] at 37°C overnight. The sections were then placed on gelatinized slides, washed in PBS, counterstained with Nuclear Fast Red, dehydrated and mounted in DPX (BDH Laboratory Supplies).

Immunohistochemistry

Tissue sections were analysed with the following antibodies: rabbit antibodies against light (L)- and heavy (H)-ferritin (Ft) [25], mouse monoclonal anti-2′,3′-cyclic nucleotide 3′-phosphodiesterase (CNPase)

© 2008 The Authors
Journal compilation © 2009 Foundation for Cellular and Molecular Medicine/Blackwell Publishing Ltd

antibody (Chemicon International, Milano, Italy), mouse monoclonal anti-neuronal nuclei (NeuN) antibody (Chemicon International), rabbit polyclonal anti-glial fibrillary acid protein (GFAP) antibody (Chemicon International), rabbit polyclonal anti- HO-1 (Stressgen, BC, Canada) antibody, rat monoclonal antimouse F4/80 antigen antibody (Serotec, Oxford, UK), rabbit polyclonal anti-human Cu–Zn superoxide dismutase-1 (SOD1) antibody (SantaCruz Biotechnology, Santa Cruz, CA, USA). Briefly, tissue sections were rehydrated in PBS, incubated in 0.3% hydrogen peroxide in PBS (RT) for 20 min., treated with 0.3% Triton-X-100 in Tris-buffered saline (TBS) for 30 min. and saturated with blocking buffer (3% milk, 10% normal swine serum in TBS) for 1 hr, followed by antibody incubation at 4°C overnight. The following biotinylated secondary antibodies were used: swine anti-rabbit IgG, rabbit anti-rat IgG and rabbit antimouse IgG (DakoCytomation, Milano, Italy). Immunoreactivity was detected with the streptABComplex/HRP system (DakoCytomation) and developed with DAB. The sections were then transferred on gelatinized slides, rinsed in PBS, counterstained with haematoxylin, dehydrated and mounted in DPX (BDH Laboratory Supplies). For double staining, the sections were stained for iron with Perl's reaction and then processed by immunohistochemistry developed with Vector SG substrate kit for peroxidase (Vector Laboratories, DBA ITALIA, Segrate, MI, Italy). Quantification of ferritin positive cells was performed as above analysing three mice for each genotype.

Immunofluorescence

Tissue sections were analysed with the following antibodies: rabbit antibodies against L- and H-Ft [25], mouse monoclonal anti-CNPase antibody (1:200; Abcam, Cambridge, UK), mouse monoclonal anti-NeuN antibody (1:100; Chemicon International), mouse monoclonal anti-GFAP antibody (1:100; Abcam), rat monoclonal antimouse F4/80 antigen antibody (1:400; Serotec). Tissue sections were rehydrated in PBS, treated with 0.1% Triton-X-100 in TBS for 30 min. and saturated with blocking buffer (10% normal goat serum in TBS) for 1 hr. Double-labelling experiments were performed by incubating the sections with a mixture of primary antibodies overnight at 4°C. The following secondary antibodies were used: fluorescein-conjugated goat anti-rabbit IgG (1:200; Sigma-Aldrich), rhodamine-conjugated goat antimouse IgG (1:250; Sigma-Aldrich), Texas red goat anti-rat IgG (Molecular Probes, Invitrogen). Sections were also labelled with 100 ng/ml 4′-6-diamidino-2-phenylindole. Sections were analysed with an Axio observed Z1 microscope (Carl Zeiss S.p.A., Arese, MI, Italy) equipped with ApoTome system for optical sectioning using a 63× objective lens.

Western blotting analysis

Protein extracts of total brain were prepared in 50 mM HEPES (N-2-hydroxyethylpiperazine-N-2-ethanesulfonic acid), 50 mM NaCl, 5 mM ethylenediaminetetraacetic acid and with protease inhibitors (aprotinin, leupeptin, pepstatin; Sigma-Aldrich). Plasma was collected from the tail vein. Fifty micrograms of total protein extracts or 0.25 μl of plasma were separated on SDS-PAGE and analysed by Western blotting according to standard protocol using antibodies against Hx (monoclonal antibody 3D6/E12), L- and H-Ft [25], Fpn1 [26], TfR1 (Zymed Laboratories Inc. South San Francisco, CA, USA), HO-1 and HO-2 (Stressgen), actin (Santa Cruz Biothecnology, Inc., Santa Cruz, CA, USA), SOD1 (SantaCruz Biotechnology) and vinculin (Sigma-Aldrich). Four mice for each genotype were analysed.

ELISA assay

Protein extracts of total brain of six wild-type and six Hx-null mice were prepared in 20 mM Tris-HCl pH 7.4, 1 mM Na Azide, 1 mM PMSF, 0.01 mM leupeptin, 0.001 mM pepstatin, 1 mM benzamidine. Brain homogenates were analysed for ferritin content by using ELISA assays based on monoclonal antibodies specific for the H-Ft (rH02) and the L-Ft (L03) calibrated on the corresponding recombinant homopolymers expressed in *E. coli* [27]. The results were expressed as nanograms of ferritin per milligrams of total brain protein ($n = 6$ for each genotype).

Quantitative realtime PCR analysis

Total liver RNA was extracted using Purelink Micro-to-Midi total RNA purification system (Invitrogen). For quantitative RealTime PCR (qRT-PCR), 1μg of total RNA was transcribed into cDNA by M-MLV reverse transcriptase (Invitrogen) and random hexamer primers (New England Biolabs, Ipswich, MA, USA). Analysis of Hepcidin mRNA levels was performed with the mouse Universal Probe Library Set (Roche) and human 18 S rRNA as endogenous control (Assays-on-Demand products from Applied Biosystems, Monza, MI, Italy). qRT-PCR was performed on a 7300 Real Time PCR System (Applied Biosystems). The qRT-PCR conditions were: 50°C for 2 min. and 95°C for 2 min., followed by 45 cycles at 95°C for 15 sec, 60°C for 30 sec and 72°C for 1 min. Six mice for each genotype were analysed.

Lipid peroxidation assay

Lipid peroxidation from tissue extracts was measured using the colorimetric assay kit Bioxytech LPO-586 from Oxis International (Portland, OR, USA) according to the manufacturer's instructions. Briefly, tissue samples were homogenized (20% wt/vol) in ice-cold 20 mM phosphate buffer (pH 7.4) containing 5 mM butylated hydroxytoluene and protein content was determined using the Biorad protein assay system (Biorad, München, Germany). Two hundred microlitres of lysate were assayed for malondialdehyde (MDA) content in hydrochloride using the chromogenic reagent N-methyl-2-phenylindole. Absorbance was measured at 586 nm and the results were expressed as pmol MDA per mg of protein ($n = 11$ for each genotype).

Statistical analysis

Results were expressed as mean ± S.E.M. Statistical analyses were performed using the Student's t-test. A *P*-value of less than 0.05 was considered significant.

Results

Iron homeostasis in haemopexin-null mice

Hx-null mice have been previously described to suffer from severe renal damage after acute intravascular haemolysis [14].

© 2008 The Authors
Journal compilation © 2009 Foundation for Cellular and Molecular Medicine/Blackwell Publishing Ltd

Table 1 Iron dosage

	Spleen	Kidney	Liver	Serum Iron
Wild-type	496.0 ± 95.88 $n = 6$	99.17 ± 12.14 $n = 9$	214.3 ± 19.77 $n = 10$	75.98 ± 2.61 $n = 6$
Hx-null	581.1 ± 92.02 $n = 7$	123.9 ± 10.78 $n = 7$	222.1 ± 22.49 $n = 10$	66.95 ± 3.38 $n = 6$
P-value	0.5361	0.1628	0.7983	0.0605

Measurement of tissue iron in the spleen, kidney, liver and serum of 2-month-old wild-type and Hx-null mice. Values are expressed as μg/g dry tissue except for serum (μg/dl).

Analysis of systemic iron metabolism showed no obvious abnormalities. Serum and tissue iron deposits were normal (Table 1). Transferrin saturation was similar in Hx-null and wild-type mice (Hx-null: 41.17% ± 5.24; wild-type: 47.33% ± 4.56; $n = 6$). Moreover, haematological parameters were in the normal range [14]. No differences were found in the hepatic expression of the iron regulatory hormone hepcidin, assayed by qRT-PCR (wild-type: 1.29 ± 0.29 *versus* Hx-null: 1.12 ± 0.26, mean ± S.E.M., $n = 6$; transcript abundance, normalized to 18 S RNA expression, is expressed as a fold increase over a calibrator sample, *i.e.* a wild-type animal).

Expression of haemopexin in brain

As several authors have reported Hx expression in the central nervous system [17, 18, 23], and Hx promoter activity was found in several brain regions in mice [20, 21], we analysed Hx expression in the mouse brain. To this end, we used the monoclonal antibody 3D6/E12 raised against a recombinant Hx lacking the first 80 amino acids of the native protein. As shown in Fig. 1A, this antibody recognizes the recombinant Hx of 42 kD in *E. coli* extracts and the mouse protein of 57 kD in the serum of wild-type animals. Western blotting analysis of total brain homogenates from 2-month-old mice, transcardially perfused with PBS, showed Hx expression in wild-type mice, and, as expected, not in Hx-null animals (Fig. 1B).

To identify the cell types expressing Hx, we performed β-galactosidase staining on brain sections of Hx-null mice as the lacZ reporter gene had been inserted into the targeting vector used to generate these animals [14]. We detected β-galactosidase activity in ependymal cells lining the ventricular system, but not in endothelial cells of the choroid plexus (Fig. 1C). A weak staining was also seen in neurons of the hippocampus (not shown).

Cellular distribution of iron deposits in haemopexin-null brain

Since Hx, by binding free heme, may participate in iron recovery [13], we analysed the cellular distribution of iron deposits (this paragraph) and ferritin (next paragraph) in brain sections of

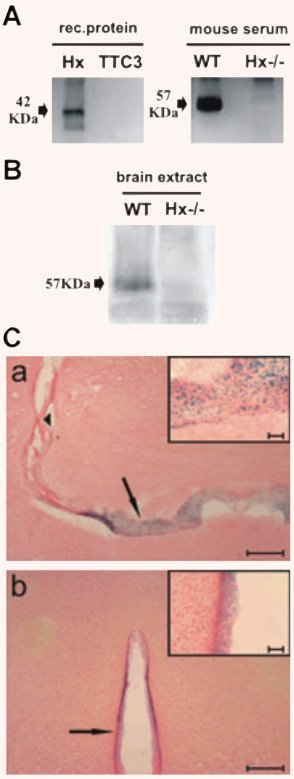

Fig. 1 Hx Expression in brain. (**A**) Western blotting analysis on cell extracts from *E. coli* expressing the recombinant Hx or the unrelated recombinant protein TTC3 (left) and on serum of a wild-type mouse and of an Hx-null mouse (right) assayed with the monoclonal antibody 3D6/E12. The antibody recognizes the recombinant Hx of 42 kD (corresponding to amino acids 81–459 of mouse Hx) and a single band of 57 kD in wild-type serum, but not in Hx-null serum. (**B**) Western blotting analysis on brain extracts of a wild-type mouse and an Hx-null mouse assayed with the monoclonal antibody 3D6/E12. Hx is detected only in wild-type sample. (**C**) Histochemical β-galactosidase detection in the brain of an Hx-null mouse. Tissues were stained with X-Gal and counterstained with nuclear fast red as reported in 'Materials and methods'. β-galactosidase activity is shown in lateral (**a**) and third (**b**) ventricles. β-galactosidase activity is restricted to ependymal cells lining the ventricular system (arrows), whereas no blue staining is detected in the epithelial cells of the choroid plexus (arrowhead). Bar = 250 μm. The insets in 'a' and 'b' show ependymal cells, stained in blue, at higher magnification (bar = 100 μm).

© 2008 The Authors
Journal compilation © 2009 Foundation for Cellular and Molecular Medicine/Blackwell Publishing Ltd

Hx-null mice compared to wild-type animals. To this end, we used the Perl's method and immunohistochemistry or immunofluorescence techniques to identify cell types accumulating iron and expressing ferritin, respectively. As expected, iron accumulated in the basal ganglia and in the thalamus in both Hx-null and wild-type mice, whereas only few scattered Perl's-positive cells could be detected in the cortex.

The analysis of Perl's-stained serial sections encompassing the basal ganglia and the thalamus, revealed an increase in the number of iron loaded cells in Hx-null mice compared to age-matched wild-type controls. Prominently affected areas included the globus pallidus and the caudate-putamen nucleus. Counts of cells positive for Perl's reaction showed that in Hx-null mice, the number of iron-loaded cells was approximately twofold greater than that of wild-type animals (Fig. 2).

To identify the cell types accumulating iron, we performed Perl's staining on brain sections followed by immunohistochemistry with antibodies against specific markers for neurons (NeuN), astrocytes (GFAP), oligodendrocytes (CNPase) and microglia (F4/80 antigen). This analysis revealed that iron accumulated mainly in oligodendrocytes of both wild-type and Hx-null mice. Occasionally, some microglial cells positive to Perl's reaction could be detected in both Hx-deficient and control mice (in less than 10% of F4/80$^+$ cells). In oligodendrocytes, iron was mainly confined to one pole of the cytoplasm and was also present in cellular processes (Fig. 3).

Cellular distribution of ferritin in haemopexin-null brain

Ferritin expression was analysed, firstly, by Western blotting on extracts from whole brain. We observed a lower expression level of H- and L-Ft in Hx-null brains than in wild-type controls (Fig. 4A). This was further confirmed by ELISA (wild-type H-Ft: 884.5 $\pm$ 8.5 ng/mg *versus* Hx-null H-Ft: 753.5 $\pm$ 7.5 ng/mg, $P < 0.01$; wild-type L-Ft: 13.45 $\pm$ 0.25 ng/mg total protein *versus* Hx-null L-Ft: 12.05 $\pm$ 0.15 ng/mg, $P < 0.05$). Then, ferritin expression was analysed by immunohistochemistry on serial sections encompassing the same regions analysed for iron deposits. In the basal ganglia and in the thalamus no differences in the number of H$^+$- or L-Ft$^+$ cells were observed between Hx-null and wild-type mice. On the other hand, we noted a decrease in the number of both H$^+$ and L-Ft$^+$ cells in the cortex of Hx-null mice compared to that of wild-type animals (Fig. 4B). To quantify this difference, H$^+$ and L-Ft$^+$ cells in the cortex (called region 'a') and in the basal ganglia and thalamus (called region 'b') were counted. There was a decrease of about 40% in the number of both H$^+$ and L-Ft$^+$ cells in the region 'a' of Hx-null mice, whereas no differences were detected in the region 'b' (Fig. 4C). The decrease in ferritin expression only in the cortex was further confirmed by Western blotting analysis on extracts from regions 'a' and 'b' (not shown).

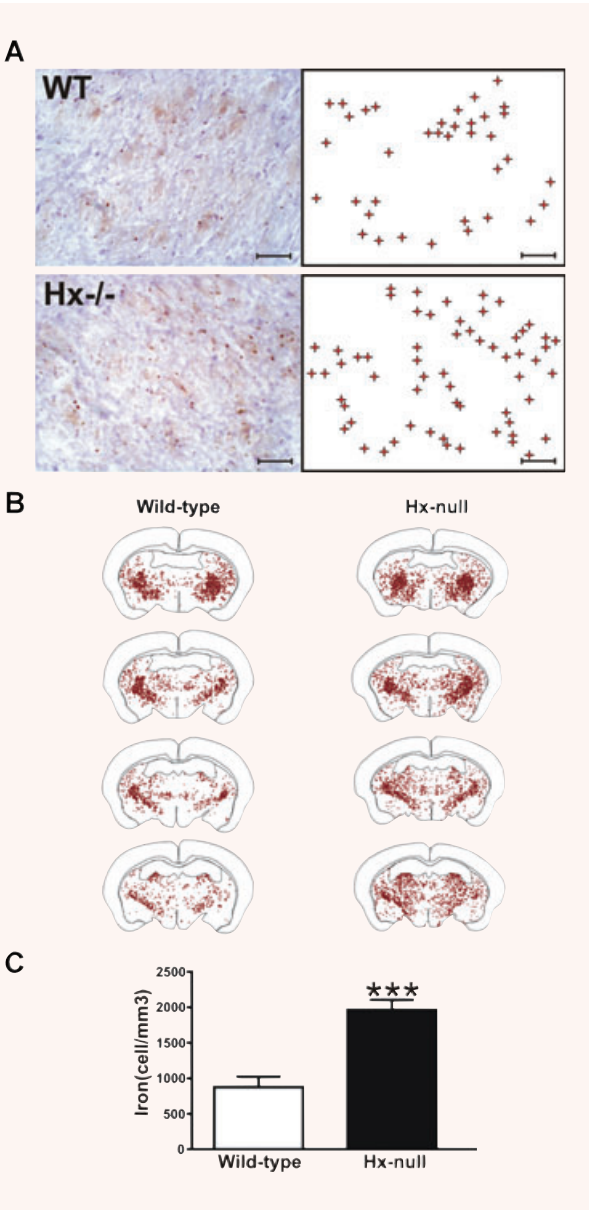

Fig. 2 Increased number of iron-loaded cells in Hx-null brain. (**A**) Brain sections of a wild-type mouse and an Hx-null mouse at 2 months of age stained with Perl's reaction and counterstained with haematoxylin. Scheme near each section represents the position of the cells positive to Perl's reaction. Bar = 100 μm. (**B**) Reconstruction of four serial sections of the brain of a wild-type mouse and an Hx-null mouse. In both mice, intense staining is evident in the basal ganglia, mainly in the globus pallidus and caudate-putamen nucleus. Hx-null mice show more iron positive cells in some thalamic regions. (**C**) Quantification of iron-loaded cells. The analysis on Perl's stained sections was performed as described in 'Materials and methods'. Data represent mean $\pm$ S.E.M., $n = 4$ mice for each genotype. *** = $P < 0.0001$.

© 2008 The Authors
Journal compilation © 2009 Foundation for Cellular and Molecular Medicine/Blackwell Publishing Ltd

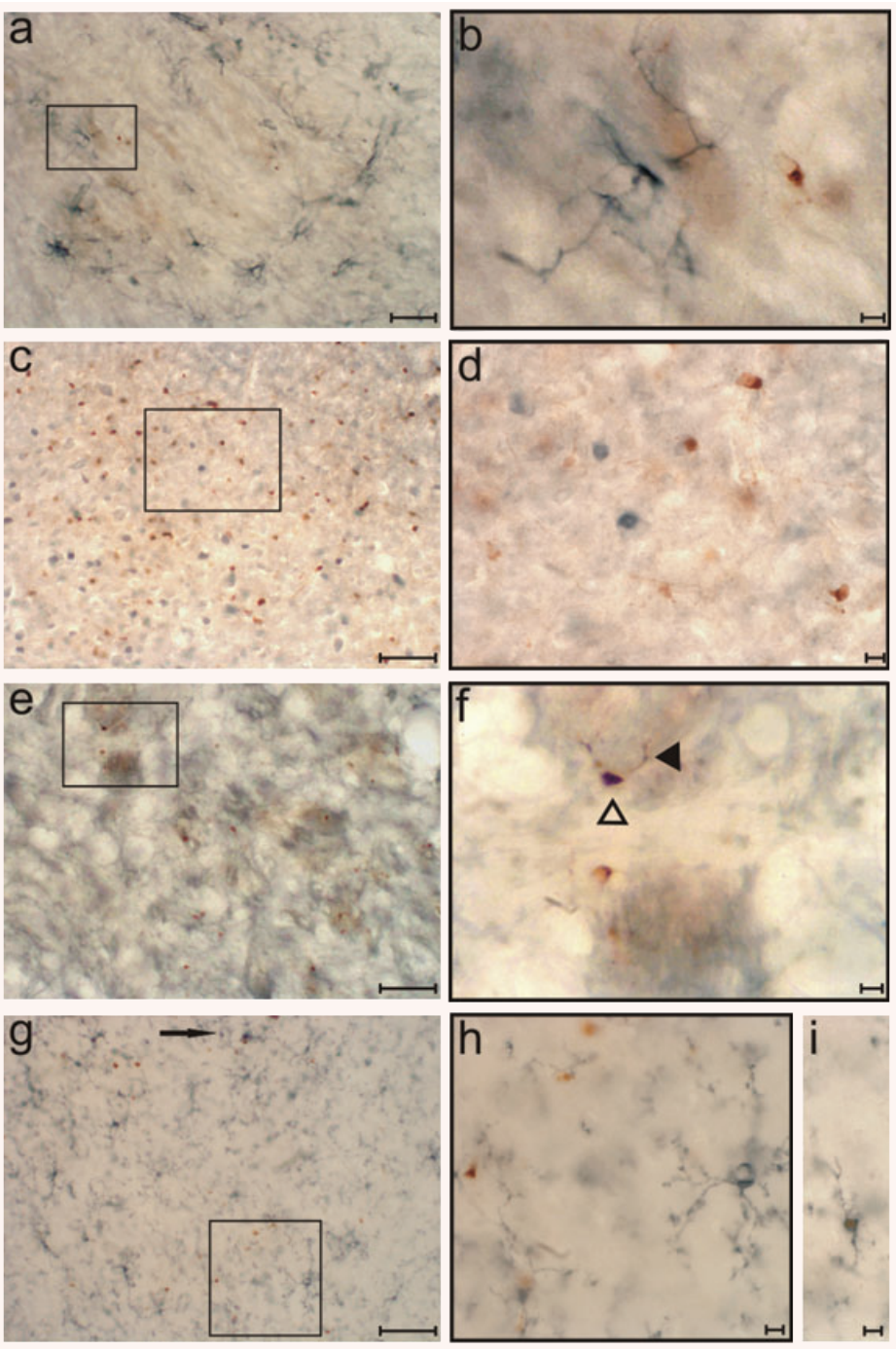

Fig. 3 Cellular localization of iron in brain. Brain sections of an Hx-null mouse stained with Perl's reaction and antibodies that recognize glial fibrillary acid protein as a marker for astrocytes (**a**, **b**), NeuN as a marker for neurons (**c**, **d**), CNPase as a marker for oligodendrocytes (**e**, **f**) and F4/80 as a marker for microglia (**g**, **h**, **i**). No astrocytes or neurons are positive for iron staining. Iron localizes specifically in oligodendrocytes and is present both in the cytosol (Δ), and in the processes (◀). Most of F4/80$^+$ cells are negative for Perl's reaction. Only few F4/80$^+$ cells contain iron in the cytosol (**i**). High power magnification of the boxes in a, c, e and g is shown in b, d, f and h, respectively; the arrow in g indicates an iron-loaded F4/80$^+$ cell, at higher magnification in i. Cellular localization of iron is the same in wild-type mice. Bars: a, c, e, g =100 μm; b, d, f, h, i = 10 μm.

To identify the cell types expressing ferritin, we performed double immunofluorescence with anti-L- or H-Ft antibodies and antibodies against specific markers for different cell populations. As shown in Fig. 5, all cell populations analysed, *i.e.* oligodendrocytes, neurons and microglia, expressed L- and H-Ft in both Hx-null and wild-type mice.

Expression of heme- iron handling molecules in haemopexin-null brain

To gain further insights into the 'iron phenotype' of Hx-null brain, we analysed the expression of molecules involved in heme-iron

© 2008 The Authors
Journal compilation © 2009 Foundation for Cellular and Molecular Medicine/Blackwell Publishing Ltd

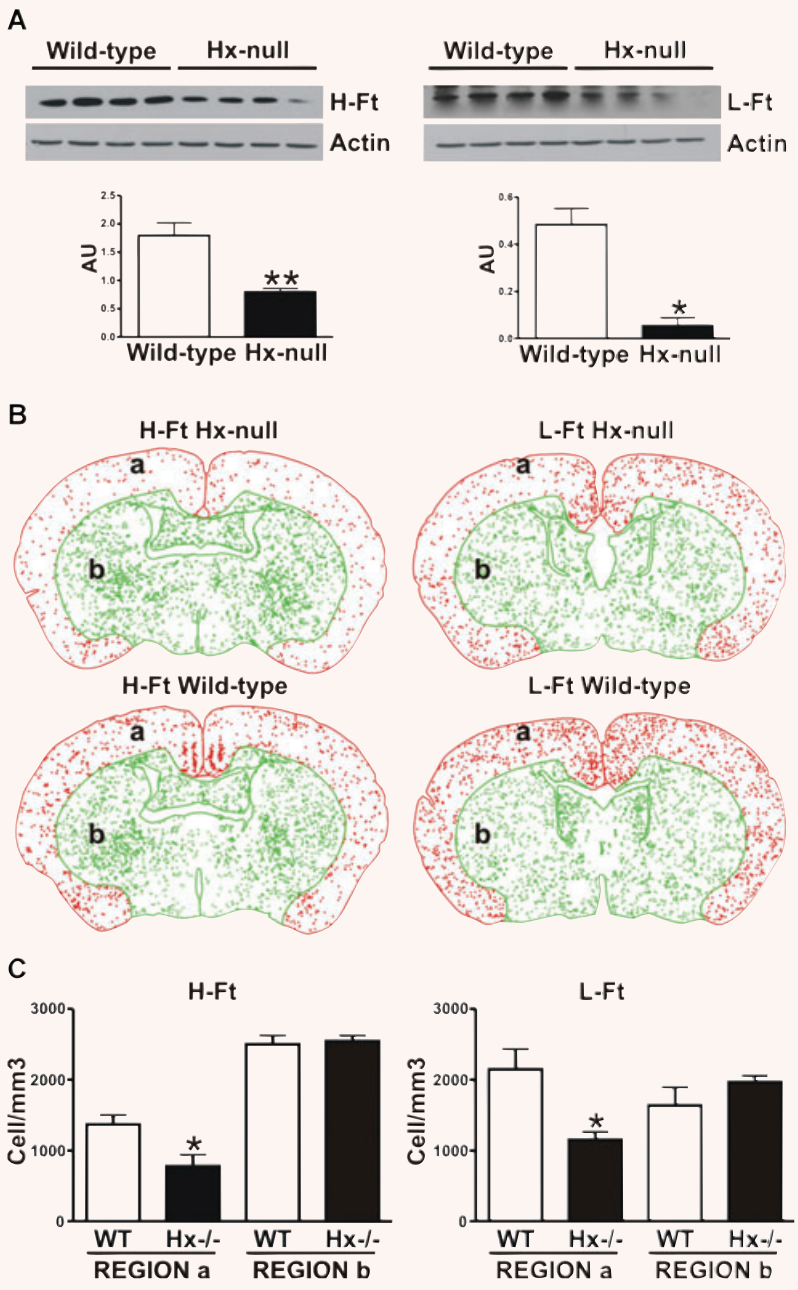

Fig. 4 Decreased expression of H- and L-Ft in Hx-null brain. (**A**) Western blotting analysis of H- and L-Ft expression in total brain extracts of four wild-type and four Hx-null mice. A representative experiment for each protein is shown. Band intensities were measured by densitometry and normalized to actin expression (AU: arbitrary unit). Densitometry data represent mean ± S.E.M.; $n = 4$ for each genotype. * = $P < 0.05$; ** = $P < 0.01$. Results shown are representative of at least three independent experiments. **(B)** Reconstruction with Neurolucida/Neuroexplorer system of two serial brain sections of an Hx-null mouse and a wild-type mouse labelled with anti H- (left) and L- Ft (right) antibodies, respectively. We marked in red the positive cells in the cerebral cortex, called region 'a', and in green the positive cells in the basal ganglia and thalamus, called region 'b'. Note the reduction in the number of H^+ and L-Ft^+ cells in the region 'a' of Hx-null mice. (C) Quantification of H^+ (left) and L-Ft^+ (right) cells shown in (**B**). Data represent mean ± S.E.M., $n = 3$ mice for each genotype. * = $P < 0.05$.

handling, *i.e.* HO-1 and HO-2 (heme degrading enzymes), TfR1 (iron acquisition system) and Fpn1 (iron exporter). This analysis was performed by Western blotting on extracts from regions 'a' and 'b' where a differential expression of L- and H-Ft was observed in Hx-null and wild-type mice. The inducible form of heme oxygenase, HO-1, was not expressed at detectable level in both Hx-null and wild-type mice. This was further confirmed by immunohistochemistry on brain sections. Moreover, no differences in the expression of HO-2, TfR1 and Fpn1 between Hx-deficient and wild-type mice neither in region 'a' or 'b' were observed (Fig. 6).

Free radical-mediated damage in haemopexin-null brain

Data presented in the previous sections showed an increase in the number of iron-loaded oligodendrocytes in the basal ganglia

© 2008 The Authors
Journal compilation © 2009 Foundation for Cellular and Molecular Medicine/Blackwell Publishing Ltd

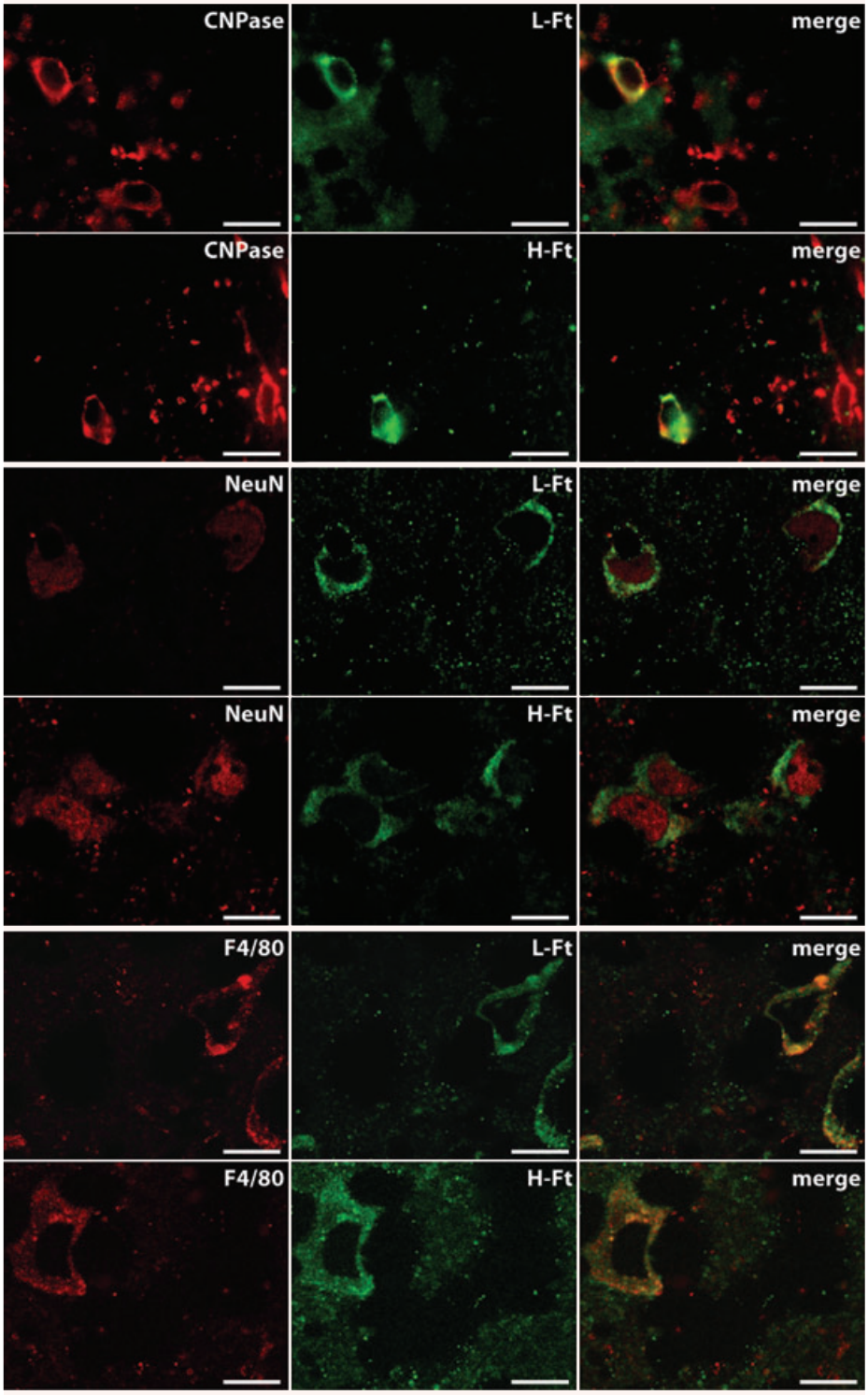

Fig. 5 Cellular localization of ferritin in brain. Brain sections of an Hx-null mouse stained by double immunofluorescence with antibodies against CNPase, NeuN, F4/80 (red) and antibodies against L- or H-Ft (green). Merged images on the right indicate that L- and H-Ft are expressed in all cell types analysed. Note that not all CNPase^{+} oligodendrocytes are positive for L- and H-Ft. Cellular localization of ferritin is the same in wild-type mice. Bars = 10 μm.

© 2008 The Authors
Journal compilation © 2009 Foundation for Cellular and Molecular Medicine/Blackwell Publishing Ltd

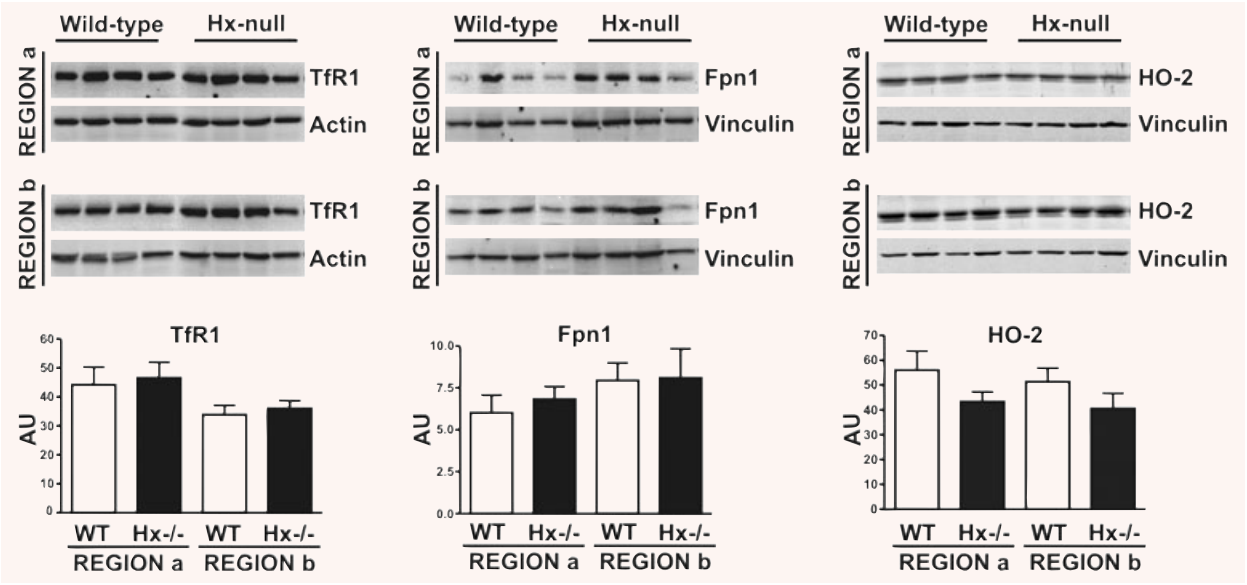

Fig. 6 HO-2, TfR1 and Fpn1 expression in brain. Western blotting analysis of TfR1 (left), Fpn1 (middle) and HO-2 (right) expression in the regions 'a' and 'b' (see Fig. 4) of four wild-type and four Hx-null mice. A representative experiment for each protein is shown. Band intensities were measured by densitometry and normalized to actin or vinculin expression (AU: arbitrary unit). Densitometry data represent mean ± S.E.M.; $n = 4$ for each genotype. Results shown are representative of at least three independent experiments.

and thalamus of Hx-null mice, not accompanied by an increase in ferritin expression. As excess iron may result in free radical generation, we measured MDA tissue level, as evidence of oxidative damage. We observed a 35% increase in brain MDA level in 2-month-old Hx-null mice compared to wild-type controls (Fig. 7A). To assess differences in oxidative stress levels between cortical and sub-cortical regions, we analysed, by immunohistochemistry, the expression of cytoplasmic SOD1 which catalyses the breakdown of superoxide radical and is induced by oxidative stress. We did not find differences in the expression of SOD1 in the region 'a' between Hx-null and wild-type mice. On the other hand, we observed a stronger expression of SOD1 in the region 'b' of Hx-null animals than in the corresponding region of wild-type controls (Fig. 7B). The increased expression of SOD1 in sub-cortical regions of Hx-null mice was further confirmed by Western blotting (Fig. 7C).

Discussion

In this paper, we report the analysis of iron deposits and ferritin expression in the brain of Hx-null mice. At the systemic level, several studies point to a role for Hx in the detoxification against heme overload [11, 14, 28, 29]. Moreover, Hx is known to be one of the most abundant proteins in CSF [23]. Nevertheless, its role in central nervous system is so far unknown.

In agreement with published data showing Hx in CSF, we found Hx protein in brain homogenates from wild-type mice. These data, together with the previously demonstrated expression of Hx mRNA in the brain [21], suggest that Hx is locally synthesized in the nervous system. Moreover, we analysed the activity of the Hx promoter in brain by detecting the expression of the lacZ gene inserted into the knock-out allele. The Hx promoter is active in the ependymal cells lining the ventricular system and, at lower level, in hippocampal neurons. The pattern of lacZ expression partially differs from previously reported data showing that a 500-bp-long fragment of the human Hx promoter is sufficient to drive the expression of β-galactosidase in several brain regions of transgenic mice, including the cortex, hippocampus, thalamus, hypothalamus, cerebellum and brainstem nuclei [20, 21]. Due to the transgene random insertion, it is possible that in those mice, lacZ expression was influenced by the genomic environment, whereas in Hx-null animals, the lacZ gene, being inserted into the genomic locus of the Hx gene, better reflects its transcriptional activity. However, due to the low sensitivity of the β-galactosidase staining, we cannot rule out the possibility that other cell types within the brain, other than hippocampal neurons, may produce Hx.

Given its ependymal expression, Hx might be released both in CSF, at the apical side of ependymal cells, and in brain parenchyma, at their basolateral side. In this way, Hx might exert a double function by scavenging heme through the ventricular system, and by protecting brain parenchyma from heme-mediated damage. Previous studies have demonstrated that the only known Hx receptor, Low-density lipoprotein receptor-related protein

© 2008 The Authors
Journal compilation © 2009 Foundation for Cellular and Molecular Medicine/Blackwell Publishing Ltd

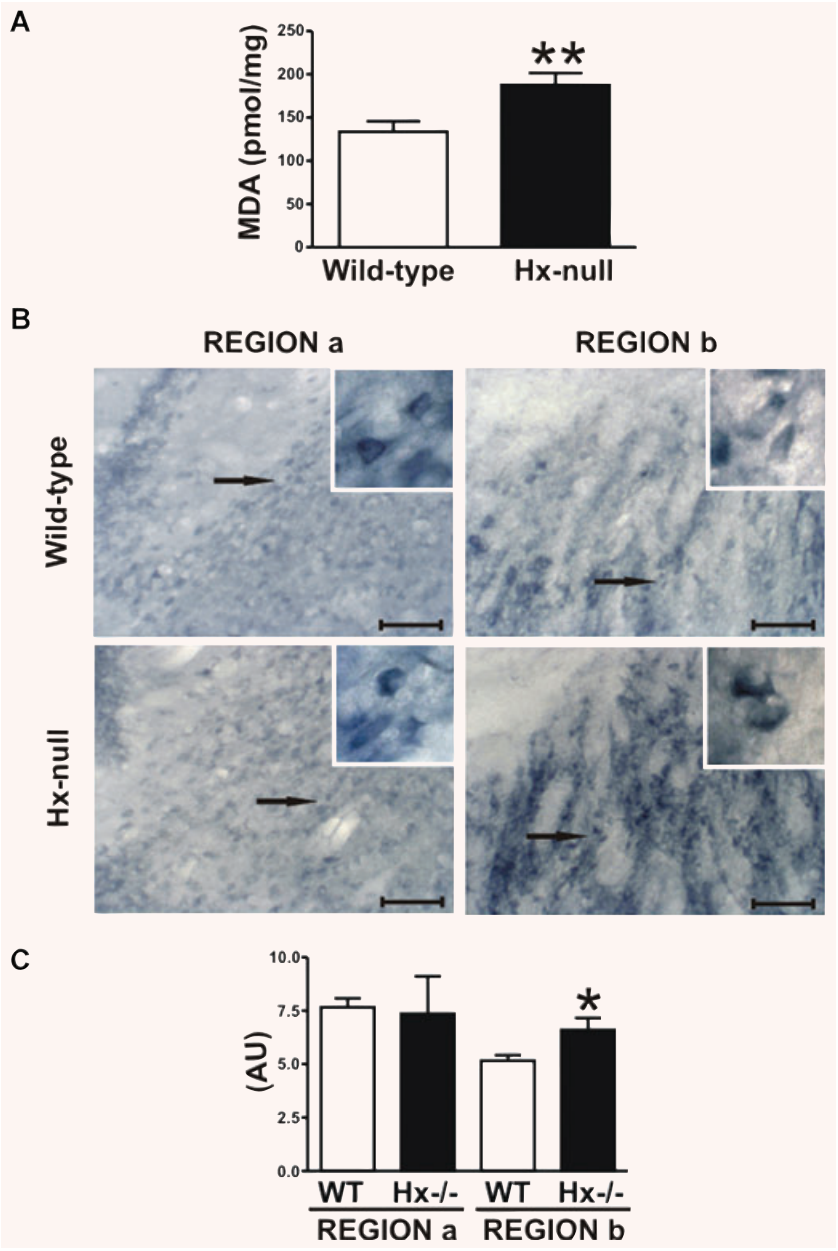

Fig. 7 Increased oxidative stress in Hx-null brain. (**A**) Lipid peroxidation, estimated as MDA levels, of total brain homogenates of wild-type and Hx-null mice. Data are shown as mean ± S.E.M.; $n = 11$ for each genotype; ** = $P < 0.01$. (**B**) Brain sections encompassing regions 'a' and 'b' (see Fig. 4) of a wild-type mouse and an Hx-null mouse stained with an antibody against SOD1. Bars = 100 μm. Arrows indicate cells shown at high magnification in the insets. Note the increased $SOD1^{+}$ signal in the region 'b' of Hx-null brain. (**C**) Densitometric analysis of a representative Western blot of SOD1 expression in the regions 'a' and 'b' of wild-type and Hx-null mice. Band intensities were measured by densitometry and normalized to vinculin expression (AU: arbitrary unit). Data represent mean ± S.E.M.; $n = 4$ for each genotype. * = $P < 0.05$. Results shown are representative of two independent experiments.

(LRP)-1 [30], is expressed in brain and, in particular, in epithelial cells of choroid plexi, neurons, glia and endothelial cells of microvessels [31–33], thus supporting the hypothesis of multiple sites of Hx activity, *i.e.* ventricular system and brain parenchyma.

Hx is known to mediate heme uptake and its degradation, through HO-1, to carbon monoxide, bilirubin and iron [8, 34, 35]. For this reason, we analysed iron deposits in brain and, because iron content within the brain varies greatly from one region to another, we focused on regions that in basal condition are characterized by highest iron concentrations. Under physiological conditions, HO-1 could not be detected in both wild-type and Hx-null mice suggesting that heme is degraded by the constitutive isoform HO-2. This is in agreement with previously reported data showing that HO-1 is strongly expressed in brain only after severe traumas [36–38].

Interestingly, we found an increased number of iron-loaded oligodendrocytes in the basal ganglia and thalamic region of Hx-null mice. Two hypotheses can explain these data, the first one being that iron overload in Hx-null mice allows the identification of oligodendrocytes that in wild-type mice are characterized by

© 2008 The Authors
Journal compilation © 2009 Foundation for Cellular and Molecular Medicine/Blackwell Publishing Ltd

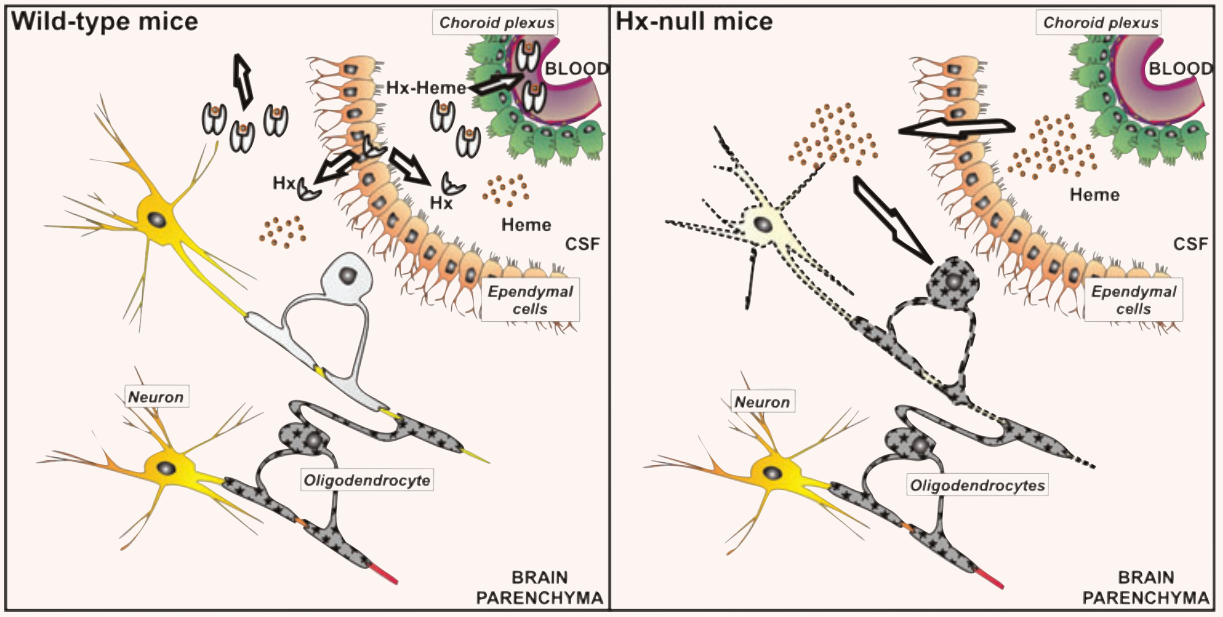

Fig. 8 A model for Hx function in brain. Hx is produced by ependymal cells and may be released both in cerebrospinal fluid and in brain parenchyma. In these compartments, Hx binds heme and the heme-Hx complexes may be taken up by cells expressing LRP-1 (see text for details). In this way, Hx contributes to maintain normal iron homeostasis in terms of iron deposits in oligodendrocytes and adequate ferritin expression (left panel). Both parameters are altered in Hx-null brain (right panel) in which we observed an increased number of iron-loaded oligodendrocytes (in grey in the figure), not accompanied by a rise in ferritin level. We hypothesize that this is due to the degradation of unbound heme out of the normal sites of heme catabolism. Excess of iron upon the storing capacity of ferritin might, in turn, cause oxidative stress and damage neurons. Colour legend: dark grey: iron-loaded oligodendrocytes; light grey: free iron oligodendrocytes; dark Yellow: neurons; light yellow: suffering neurons.

undetectable iron levels. Alternatively, in Hx-null mice excess of iron might be stored in a subpopulation of oligodendrocytes that normally does not participate in iron metabolism. Indeed, the presence of specific subsets of oligodendrocytes, also in relation to iron metabolism, has already been demonstrated [1, 39]. Accordingly, immunofluorescence experiments performed in this work have revealed the presence of oligodendrocytes that do not express ferritin both in wild-type and in Hx null mice.

Hx-null mice showed a significant decrease in H- and L-Ft expression levels in total brain extract. However, the regulation of H- and L-Ft expression was region specific and not pertaining to the whole brain, as demonstrated by the immunohistochemical analyses. The areas that were mainly involved in iron accumulation did not show a rise in ferritin level. This condition is common to several human neurological disorders such as Alzheimer's disease and Parkinson's disease in which iron loading is not associated with an adequate increase in ferritin expression [4]. Moreover, it is well documented that ferrous iron, not stored in ferritin, modulates oxidative injury by generating the hydroxyl radical *via* Fenton reaction [40]. Accordingly, we showed that Hx-null brain was characterized by higher levels of lipid peroxidation, indicative of oxidative stress, than wild-type controls. Analysis of SOD1 demonstrated that oxidative stress was limited to subcortical regions where iron loading was not associated to an increase in ferritin.

On the other hand, in the cerebral cortex of Hx-null mice, there was a strong reduction of H^+ and L-Ft^+ cells that might reflect a decrease in total cell number or a down-regulation of ferritin expression in cell populations within this region. The latter might be indicative of decreased iron stores. Nevertheless, we did not find differences between Hx-null and wild-type mice in Perl's staining pattern in the cortex or in SOD1 expression in this region. So, it is possible that other mechanisms, not directly related to iron level, might be responsible for decreased ferritin expression in Hx-null cortex. Accordingly, it has been demonstrated that several stimuli regulate at transcriptional level ferritin biosynthesis [41].

Beside from ferritins, other molecules involved in the transport of iron ions like TfR1 and Fpn1 did not show alterations in the expression level, thus suggesting that the difference in ferritin expression might not be directly related to a difference in Tf-bound iron acquisition or in iron export from cells. Thus, it is possible that other molecules involved in heme trafficking might be responsible for the differences in iron deposits and ferritin expression observed in Hx-null mice. Accordingly, both the heme importer heme carrier protein-1, and the heme exporters, ATP-binding

© 2008 The Authors
Journal compilation © 2009 Foundation for Cellular and Molecular Medicine/Blackwell Publishing Ltd

cassette (ABC)G2 and feline leukaemia virus subgroup C cellular receptor (FLVCR), are strongly expressed in brain [42–45].

In conclusion, we identified the sites of Hx expression in brain that point to a role of Hx in both CSF and brain parenchyma as illustrated in Fig. 8. In wild-type mice the heme-Hx complex may be taken up by several cell types expressing LRP-1 including epithelial cells of choroid plexi, endothelial cells of vessels, neurons and glial cells [31–33]. In Hx-null mice heme catabolism out of canonical sites results in an increase in the number of iron loaded oligodendrocytes in the basal ganglia and thalamus not accompanied by an increase in H- and L-Ft expression. This might, in turn, generate free radical responsible for cell damage. Further studies are needed to elucidate the molecular mechanisms underlying this situation.

In human brain, iron misregulation is an hallmark of trauma, ischemia and neurodegenerative disorders [46–49]. Our results suggest that Hx may modulate trauma resolution and/or the evolution of neurodegenerative diseases.

Acknowledgements

We thank Sonia Levi for the gift of anti-ferritin antibodies and David Haile for anti-Ferroportin antibody. We thank Paolo Santambrogio for performing ELISA experiment. We are grateful to Flavia Favilla and Simonetta Geninatti Crich for help with some experiments and to Samuele Marro and Deborah Chiabrando for assistance with manuscript preparation. This work was supported by the Italian Ministry of University and Research to E.T. and F.A., by 'Regione Piemonte' to F.A. and by 'Compagnia di San Paolo' to A.V.
Conflict of interest: none declared.

References

1. **Connor JR, Menzies SL.** Relationship of iron to oligodendrocytes and myelination. *Glia*. 1996; 17: 83–93.
2. **Curtis AR, Fey C, Morris CM, *et al.*** Mutation in the gene encoding ferritin light polypeptide causes dominant adult-onset basal ganglia disease. *Nat Genet*. 2001; 28: 350–4.
3. **Patel PI, Isaya G.** Friedreich ataxia: from GAA triplet-repeat expansion to frataxin deficiency. *Am J Hum Genet*. 2001; 69: 15–24.
4. **Zecca L, Youdim MB, Riederer P, *et al.*** Iron, brain ageing and neurodegenerative disorders. *Nat Rev Neurosci*. 2004; 5: 863–73.
5. **Tolosano E, Altruda F.** Hemopexin: structure, function, and regulation. *DNA Cell Biol*. 2002; 21: 297–306.
6. **Davies DM, Smith A, Muller-Eberhard U, *et al.*** Hepatic subcellular metabolism of heme from heme-hemopexin: incorporation of iron into ferritin. *Biochem Biophys Res Commun*. 1979; 91: 1504–11.
7. **Smith A, Morgan WT.** Haem transport to the liver by haemopexin. Receptor-mediated uptake with recycling of the protein. *Biochem J*. 1979; 182: 47–54.
8. **Eskew JD, Vanacore RM, Sung L, *et al.*** Cellular protection mechanisms against extracellular heme. heme-hemopexin, but not free heme, activates the N-terminal c-jun kinase. *J Biol Chem*. 1999; 274: 638–48.
9. **Smith A, Alam J, Escriba PV, *et al.*** Regulation of heme oxygenase and metallothionein gene expression by the heme analogs, cobalt-, and tin-protoporphyrin. *J Biol Chem*. 1993; 268: 7365–71.
10. **Gutteridge JM, Smith A.** Antioxidant protection by haemopexin of haem-stimulated lipid peroxidation. *Biochem J*. 1988; 256: 861–5.
11. **Vinchi F, Gastaldi S, Silengo L, *et al.*** Hemopexin prevents endothelial damage and liver congestion in a mouse model of heme overload. *Am J Pathol*. 2008; 173: 289–99.
12. **Ascenzi P, Bocedi A, Visca P, *et al.*** Hemoglobin and heme scavenging. *IUBMB Life*. 2005; 57: 749–59.
13. **Hershko C.** The fate of circulating haemoglobin. *Br J Haematol*. 1975; 29: 199–204.
14. **Tolosano E, Hirsch E, Patrucco E, *et al.*** Defective recovery and severe renal damage after acute hemolysis in hemopexin-deficient mice. *Blood*. 1999; 94: 3906–14.
15. **Tolosano E, Fagoonee S, Hirsch E, *et al.*** Enhanced splenomegaly and severe liver inflammation in haptoglobin/hemopexin double-null mice after acute hemolysis. *Blood*. 2002; 100: 4201–8.
16. **Camborieux L, Julia V, Pipy B, *et al.*** Respective roles of inflammation and axonal breakdown in the regulation of peripheral nerve hemopexin: an analysis in rats and in C57BL/WIds mice. *J Neuroimmunol*. 2000; 107: 29–41.
17. **Madore N, Camborieux L, Bertrand N, *et al.*** Regulation of hemopexin synthesis in degenerating and regenerating rat sciatic nerve. *J Neurochem*. 1999; 72: 708–15.
18. **Morris CM, Candy JM, Edwardson JA, *et al.*** Evidence for the localization of haemopexin immunoreactivity in neurones in the human brain. *Neurosci Lett*. 1993; 149: 141–4.
19. **Swerts JP, Soula C, Sagot Y, *et al.*** Hemopexin is synthesized in peripheral nerves but not in central nervous system and accumulates after axotomy. *J Biol Chem*. 1992; 267: 10596–600.
20. **Chiocchetti A, Tolosano E, Hirsch E, *et al.*** Green fluorescent protein as a reporter of gene expression in transgenic mice. *Biochim Biophys Acta*. 1997; 1352: 193–202.
21. **Tolosano E, Cutufia MA, Hirsch E, *et al.*** Specific expression in brain and liver driven by the hemopexin promoter in transgenic mice. *Biochem Biophys Res Commun*. 1996; 218: 694–703.
22. **Castano EM, Roher AE, Esh CL, *et al.*** Comparative proteomics of cerebrospinal fluid in neuropathologically-confirmed Alzheimer's disease and non-demented elderly subjects. *Neurol Res*. 2006; 28: 155–63.
23. **Davidsson P, Folkesson S, Christiansson M, *et al.*** Identification of proteins in human cerebrospinal fluid using liquid-phase isoelectric focusing as a prefractionation step followed by two-dimensional gel electrophoresis and matrix-assisted laser desorption/ionisation mass spectrometry. *Rapid Commun Mass Spectrom*. 2002; 16: 2083–8.
24. **Pieroni L, Khalil L, Charlotte F, *et al.*** Comparison of bathophenanthroline sulfonate and ferene as chromogens in colorimetric measurement of low hepatic iron concentration. *Clin Chem*. 2001; 47: 2059–61.
25. **Santambrogio P, Cozzi A, Levi S, *et al.*** Functional and immunological analysis of recombinant mouse H- and L-ferritins

© 2008 The Authors
Journal compilation © 2009 Foundation for Cellular and Molecular Medicine/Blackwell Publishing Ltd

from Escherichia coli. *Protein Expr Purif*. 2000; 19: 212–8.
26. **Abboud S, Haile DJ.** A novel mammalian iron-regulated protein involved in intracellular iron metabolism. *J Biol Chem*. 2000; 275: 19906–12.
27. **Cozzi A, Levi S, Bazzigaluppi E, *et al*.** Development of an immunoassay for all human isoferritins, and its application to serum ferritin evaluation. *Clin Chim Acta*. 1989; 184: 197–206.
28. **Balla J, Vercellotti GM, Jeney V, *et al*.** Heme, heme oxygenase and ferritin in vascular endothelial cell injury. *Mol Nutr Food Res*. 2005; 49: 1030–43.
29. **Kumar S, Bandyopadhyay U.** Free heme toxicity and its detoxification systems in human. *Toxicol Lett*. 2005; 157: 175–88.
30. **Hvidberg V, Maniecki MB, Jacobsen C, *et al*.** Identification of the receptor scavenging hemopexin-heme complexes. *Blood*. 2005; 106: 2572–9.
31. **Donahue JE, Flaherty SL, Johanson CE, *et al*.** RAGE, LRP-1, and amyloid-beta protein in Alzheimer's disease. *Acta Neuropathol*. 2006; 112: 405–15.
32. **Shibata M, Yamada S, Kumar SR, *et al*.** Clearance of Alzheimer's amyloid-ss(1–40) peptide from brain by LDL receptor-related protein-1 at the blood-brain barrier. *J Clin Invest*. 2000; 106: 1489–99.
33. **Zhang X, Polavarapu R, She H, *et al*.** Tissue-type plasminogen activator and the low-density lipoprotein receptor-related protein mediate cerebral ischemia-induced nuclear factor-kappaB pathway activation. *Am J Pathol*. 2007; 171: 1281–90.
34. **Sung L, Shibata M, Eskew JD, *et al*.** Cell-surface events for metallothionein-1 and heme oxygenase-1 regulation by the hemopexin-heme transport system. *Antioxid Redox Signal*. 2000; 2: 753–65.
35. **Vanacore RM, Eskew JD, Morales PJ, *et al*.** Role for copper in transient oxidation and nuclear translocation of MTF-1, but not of NF-kappa B, by the heme-hemopexin transport system. *Antioxid Redox Signal*. 2000; 2: 739–52.
36. **Stahnke T, Stadelmann C, Netzler A, *et al*.** Differential upregulation of heme oxygenase-1 (HSP32) in glial cells after oxidative stress and in demyelinating disorders. *J Mol Neurosci*. 2007; 32: 25–37.
37. **Yan W, Wang HD, Hu ZG, *et al*.** Activation of Nrf2-ARE pathway in brain after traumatic brain injury. *Neurosci Lett*. 2008; 431: 150–4.
38. **Park C, Cho IH, Kim D, *et al*.** Toll-like receptor 2 contributes to glial cell activation and heme oxygenase-1 expression in traumatic brain injury. *Neurosci Lett*. 2008; 431: 123–8.
39. **Espinosa de los Monteros A, de Vellis J.** Myelin basic protein and transferrin characterize different subpopulations of oligodendrocytes in rat primary glial cultures. *J Neurosci Res*. 1988; 21: 181–7.
40. **Meneghini R.** Iron homeostasis, oxidative stress, and DNA damage. *Free Radic Biol Med*. 1997; 23: 783–92.
41. **Torti FM, Torti SV.** Regulation of ferritin genes and protein. *Blood*. 2002; 99: 3505–16.
42. **Cooray HC, Blackmore CG, Maskell L, *et al*.** Localisation of breast cancer resistance protein in microvessel endothelium of human brain. *Neuroreport*. 2002; 13: 2059–63.
43. **Eisenblatter T, Huwel S, Galla HJ.** Characterisation of the brain multidrug resistance protein (BMDP/ABCG2/BCRP) expressed at the blood-brain barrier. *Brain Res*. 2003; 971: 221–31.
44. **Inoue K, Nakai Y, Ueda S, *et al*.** Functional characterization of PCFT/HCP1 as the molecular entity of the carrier-mediated intestinal folate transport system in the rat model. *Am J Physiol-Gastr L*. 2008; 294: G660–8.
45. **Keel SB, Doty RT, Yang Z, *et al*.** A heme export protein is required for red blood cell differentiation and iron homeostasis. *Science*. 2008; 319: 825–8.
46. **Berg D, Hochstrasser H.** Iron metabolism in Parkinsonian syndromes. *Mov Disord*. 2006; 21: 1299–310.
47. **Berg D, Youdim MB.** Role of iron in neurodegenerative disorders. *Top Magn Reson Imaging*. 2006; 17: 5–17.
48. **Gregory A, Hayflick SJ.** Neurodegeneration with brain iron accumulation. *Folia Neuropathol*. 2005; 43: 286–96.
49. **Selim MH, Ratan RR.** The role of iron neurotoxicity in ischemic stroke. *Ageing Res Rev*. 2004; 3: 345–53.

© 2008 The Authors
Journal compilation © 2009 Foundation for Cellular and Molecular Medicine/Blackwell Publishing Ltd